

Characteristic Energy Losses of 8-keV Electrons in Liquid Al, Bi, In, Ga, Hg, and Au*

C. J. POWELL

National Bureau of Standards, Washington, District of Columbia 20234

(Received 14 June 1968)

Characteristic loss spectra have been obtained in a reflection scattering geometry for liquid Al, Bi, In, Ga, Hg, and Au and, in the case of Al, Bi, and Au, for the same specimens in the solid phase. Peaks due to surface and volume plasmon excitation dominated the loss spectra for all elements except Au. The relative intensity of these peaks varied rapidly with scattering angle for the Al, Bi, In, and Ga specimens, but there was little angular variation when Al, Bi, or Au was evaporated onto a frozen substrate of the same element. The Al plasmon losses varied with temperature and changed at the melting point as would be expected from the known density variation. Changes in the Bi plasmon energy losses on melting and changes in other structure on melting have been interpreted in terms of band-structure changes. The peaks in the gold loss spectra appeared to become broader and less distinct on melting, from which it was concluded that the Au excited states had shorter lifetimes with increased disorder. In general, however, the liquid- and solid-state spectra of the same element were similar, thereby showing that for these materials there was not a large change in the electronic structure on melting.

I. INTRODUCTION

IN recent years, there has been interest in the electronic structure of liquids, particularly liquid metals, and of any difference in the electronic properties in the solid and liquid states of particular materials.¹ The work reported here was undertaken to find to what extent the characteristic energy losses² of 8-keV electrons in certain solids changed on melting and to relate the observed liquid-state spectra to other relevant liquid properties.

A. Possible Changes in Characteristic Loss Spectra on Melting

The characteristic electron energy loss spectra of solids have been successfully interpreted in terms of the macroscopic dielectric constant $\epsilon(\omega, k)$, a function of frequency ω and wave number k .² In this paper we will be concerned only with the appearance and location of prominent structure in energy loss spectra which are primarily related to the frequency variation of $\epsilon(\omega, k)$. It will be convenient to use the following expression³ for $\epsilon(\omega, 0)$:

$$\epsilon(\omega, 0) = 1 - \frac{f_0 \omega_p^2}{\omega^2 + i g_0 \omega} - \sum_{j=1}^n \frac{f_j \omega_p^2}{\omega^2 - \omega_j^2 + i g_j \omega}, \quad (1)$$

where

$$\omega_p = (4\pi N e^2 / m)^{1/2} \quad (2)$$

and N is the valence electron density, $f_0 = m/m^*$ is an oscillator strength that describes the free-electron contribution to $\epsilon(\omega, 0)$, and g_0 is the reciprocal of the re-

laxation time of electrons in the valence band. The effective mass m^* is the optical effective mass defined by Cohen.⁴ The last term in Eq. (1) represents the contribution to $\epsilon(\omega, 0)$ of interband transitions of frequency ω_j , oscillator strength f_j , and of lifetime $1/g_j$. For primary electron energies in the keV range and for relatively small energy losses, the characteristic loss spectrum in an infinite medium is defined principally by $-\text{Im}[1/\epsilon(\omega, 0)]$;² effects due to the k dependence of $-\text{Im}[1/\epsilon(\omega, k)]$ are not significant in most of the present work. An energy loss $\Delta E_v = \hbar\omega_v$ due to "volume" plasmon⁵ excitation may occur for a frequency ω_v near $\epsilon(\omega) = 0$. Further energy losses due to interband transitions may also be observed at positions near those $\hbar\omega_j$ with significant oscillator strength. In addition, at a solid-vacuum interface a "surface" plasmon⁶ loss $\Delta E_s = \hbar\omega_s$ may occur for a frequency ω_s , where $-\text{Im}\{1/[1 + \epsilon(\omega)]\}$ is a maximum near $\epsilon_1(\omega) = -1$ and where $\epsilon(\omega) = \epsilon_1(\omega) + i\epsilon_2(\omega)$.

It should be possible to apply the formalism described briefly above to liquids⁷ and it will be desirable to make a distinction between the dielectric constants $\epsilon_{\text{sol}}(\omega)$ and $\epsilon_{\text{liq}}(\omega)$ for the solid and liquid states of a given material. Differences between $\epsilon_{\text{sol}}(\omega)$ and $\epsilon_{\text{liq}}(\omega)$ could lead to differences in the loss spectra for the solid and liquid states in the following ways.

(a) For materials in which the contribution of interband transitions to $\epsilon_{\text{sol}}(\omega)$ and $\epsilon_{\text{liq}}(\omega)$ is small for frequencies $\omega \approx \omega_p$, strong volume and surface plasmon loss peaks would be expected at positions ΔE_v and ΔE_s near $\hbar\omega_p$ and $\hbar\omega_p/\sqrt{2}$, respectively. Since ω_p is a function of density [Eq. (2)], it would be expected that ΔE_v and ΔE_s would vary smoothly with temperature in the solid and liquid states and that there could be a discontinuity at the melting point consistent with any density change on melting.

⁴ M. H. Cohen, *Phil. Mag.* **3**, 762 (1958).

⁵ D. Pines, *Rev. Mod. Phys.* **28**, 184 (1956).

⁶ R. H. Ritchie, *Phys. Rev.* **106**, 874 (1957); E. A. Stern and R. A. Ferrell, *ibid.* **120**, 130 (1960).

⁷ U. Fano, *Phys. Rev.* **102**, 1202 (1956).

* Work carried out at the National Bureau of Standards under the sponsorship of the U. S. Atomic Energy Commission, Division of Biology and Medicine.

¹ N. E. Cusack, *Rept. Progr. Phys.* **26**, 361 (1963); *Advan. Phys.* **16**, No. 62 (1967); **16**, No. 63 (1967); **16**, No. 64 (1967).

² The most comprehensive recent review of theory and experiment concerning characteristic energy losses of electrons in solids has been published by H. Raether, *Springer Tracts in Modern Physics* (Springer-Verlag, Berlin, 1965), Vol. 38, p. 84.

³ See, e.g., F. Seitz, in *The Modern Theory of Solids* (McGraw-Hill Book Co., New York, 1940), Chap. 17.

(b) For materials in which the structure in $-\text{Im}[1/\epsilon(\omega)]$ is due principally to interband transitions and where ϵ_2 is large (compared to unity) so that the plasmon resonances are broad and poorly defined, any observed differences in the loss spectra for the solid and liquid states can be related directly to changes in the interband transition frequencies ω_j or the oscillator strengths f_j and hence in the band structure.

(c) In cases when one or more interband transitions occur with frequency ω_j close to ω_p or $\omega_p/\sqrt{2}$, the observed plasmon losses ΔE_v and ΔE_s may be shifted significantly from $\hbar\omega_p$ and $\hbar\omega_p/\sqrt{2}$. Such shifts may occur even though the particular f_j may be too small for an energy loss peak (near $\hbar\omega_j$) due to the interband transition to be observed directly.^{8,9} Changes in the differences $\Delta E_v - \hbar\omega_p$ and $\Delta E_s - \hbar\omega_p/\sqrt{2}$ for a material on melting may then be due to a change in the ω_j or the f_j ; such changes would also be evidence of changes in the band structure on melting.

(d) The lack of long-range order in the liquid phase might lead to changes in band structure (with effects as predicted above) or to increases in g_0 and g_j with corresponding increases in the widths of the observed loss peaks.

B. Review of Previous Experiments

Several measurements of characteristic losses of kilovolt electrons in liquid metals have been reported.¹⁰⁻¹³ Boersch *et al.*¹⁰ compare the loss spectra of mercury in the solid, liquid, and vapor states and emphasize the similarity in the spectra for the three phases. They find a sharp loss peak at 6.3 eV in the solid and a narrower peak at 6.4 eV in the liquid phase. A broader peak is observed in the solid at 13.0 eV (which may be due at least in part to two scatterings involving the 6.3-eV loss) while a second peak is also observed in the liquid at 10.8 eV. From measurements of $\epsilon_{\text{liq}}(\omega)$ for Hg by Wilson and Rice¹⁴ it would be expected that ΔE_v should be about 7 eV and ΔE_s about 6 eV; in the transmission experiment of Boersch *et al.* the 6.4-eV loss is probably due to volume plasmon excitation. On the basis of density-change⁵ considerations [Eq. (2)], the plasmon losses should be larger in the solid than in the liquid though the new structure observed at 10.8 eV in liquid Hg will also tend to lower ΔE_v compared to the value in the solid.⁸ The observed loss, however, is slightly larger in the liquid than in the solid and this observation is therefore inconsistent with the prediction made above. Also, no significant structure in $-\text{Im}[1/\epsilon_{\text{liq}}(\omega)]$ in the vicinity of 10.8 eV is found using

the optical data of Wilson and Rice.¹⁴ The loss spectrum of liquid Hg should therefore be remeasured to resolve this discrepancy.

Arifov and Kasymov¹¹ have reported that the characteristic loss spectra of Sn and In do not change on melting. Their characteristic losses for Sn unfortunately do not agree at all well with those measured using evaporated Sn specimens¹⁵ and it is surmised that the measured loss spectra do not represent the properties of liquid or solid Sn. Experimental curves or loss values for In are not shown in this paper.

A new series of experiments has been performed to determine the characteristic loss spectra of certain liquids and to compare them with the spectra of the corresponding solids. It was hoped to relate any changes in the spectra for the solid and liquid states to the hypotheses listed above and to see whether there was any detectable change in the spectrum of electronic excitations on melting. A brief report has been given of changes in the loss spectrum of solid Bi on melting.¹² It was found that a peak at 11.5-eV energy loss (due presumably to an interband transition) in the spectrum of liquid Bi did not occur in the solid Bi spectrum, and that a peak at 5.3-eV loss in the solid Bi spectrum did not appear in the liquid Bi spectrum. Also, the changes in ΔE_v and ΔE_s on melting could not be related to the known density change,¹⁶ as discussed in hypothesis (c) above. These observations were regarded as an indication of a change in the Bi band structure on melting. The work has also been extended to measurements of characteristic energy losses in a series of liquid In-Bi and In-Al alloys.¹³ Plasmon loss peaks ΔE_v and ΔE_s were observed in each liquid alloy but the variation with composition could not be simply related to density changes. The deviations from the variation expected by assuming the last term in Eq. (1) to be zero were interpreted in terms of the composition variation of one or more interband transitions with frequencies $\omega_j \sim \omega_p$. It was assumed that there was only one interband transition of significance in the range of interest [that is, $n=1$ in Eq. (1)] and it was then possible to compute $\hbar\omega_1$ and f_1 for bismuth-rich In-Bi alloys and indium-rich In-Al alloys.

In the present paper, measurements of the loss spectra of 8-keV electrons scattered by liquid Al, Bi, In, Ga, Hg, and Au using a "reflection" geometry will be presented and discussed. These elements were convenient for study because their vapor pressures at their melting points (room temperature for Hg) were low enough to permit satisfactory measurement.¹⁷ For Al, Bi, and Au, comparisons were made with the energy loss spectra recorded with the same specimen in the solid phase. In addition, spectra were recorded for Al,

⁸ C. B. Wilson, Proc. Phys. Soc. (London) **76**, 481 (1960).

⁹ C. J. Powell (unpublished).

¹⁰ H. Boersch, J. Geiger, H. Hellwig, and H. Michel, Z. Physik **169**, 252 (1962).

¹¹ U. A. Arifov and A. Kh. Kasymov, Dokl. Akad. Nauk SSSR **158**, 82 (1964) [English transl.: Soviet Phys.-Doklady **9**, 789 (1965)].

¹² C. J. Powell, Phys. Rev. Letters **15**, 852 (1965).

¹³ C. J. Powell, Advan. Phys. **16**, 203 (1967).

¹⁴ E. G. Wilson and S. A. Rice, Phys. Rev. **145**, 55 (1966).

¹⁵ C. J. Powell, Proc. Phys. Soc. (London) **76**, 593 (1960).

¹⁶ *Liquid Metals Handbook*, edited by C. B. Jackson (U. S. Atomic Energy Commission and U. S. Navy, Washington, D. C., 1955).

¹⁷ R. E. Honig, R. C. A. Rev. **23**, 567 (1962).

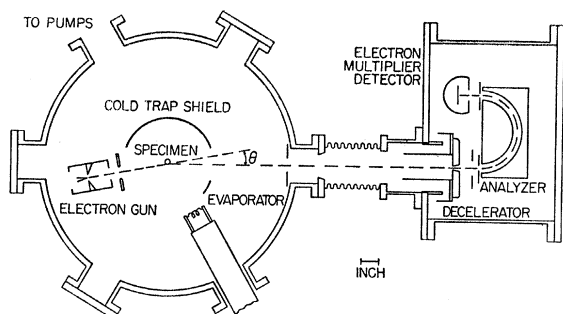


FIG. 1. Schematic outline of the apparatus.

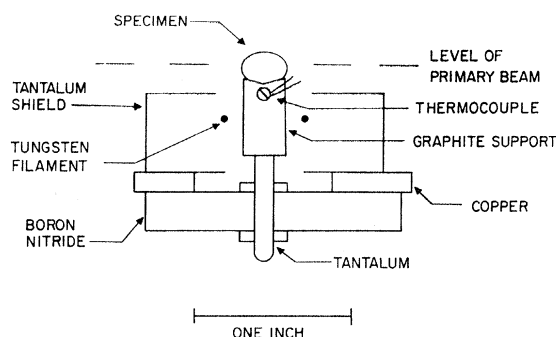


FIG. 2. Section through the specimen holder.

Bi, and Au evaporated onto frozen Al, Bi, and Au substrates, respectively.

II. EXPERIMENTAL

A schematic outline of the apparatus is shown in Fig. 1 and the specimen assembly is shown in more detail in Fig. 2. The electron beam of 8-keV energy is produced by a Steigerwald¹⁸ gun that can be rotated about a vertical axis through the specimen which is at ground potential. Material can be evaporated if desired from a helical tungsten filament or a conical basket onto the specimen surface. The target is surrounded by a shield that is part of a liquid-nitrogen reservoir to minimize carbonaceous contamination on surfaces under electron bombardment.¹⁹

Electrons scattered through an angle θ in the surface region of the specimen were decelerated to a standard energy of 45 eV using half of a filter lens²⁰ as a short-focus decelerator. The decelerated beam was dispersed by a hemispherical condenser²¹ and detected with an electron multiplier, the output pulse rate being displayed on an X-Y recorder as a function of a variable sweep voltage applied to the gun cathode. With the gun pointing into the analyzer, the measured energy resolution was about 0.8 eV full width at half-maximum and the angular resolution 1–3 mrad, depending on the gun bias and the location of the tungsten hairpin filament. The half-width of the peak due to electrons scattered elastically by the specimen, however, was between 1.0 and 1.6 eV (varying with the specimen topography and the system alignment). Calibration of the recorded spectra was performed by inserting a known potential difference V_0 (where eV_0 was comparable to an energy loss to be measured) from a group of mercury batteries in series with the gun cathode, thereby shifting the elastic peak on the record.

The specimens were supported on a graphite post (Fig. 2). Graphite was chosen for this purpose because

it is not wetted by and does not significantly react with the six liquids studied here for the usual operating temperatures and times.^{16,22} The graphite post was heated by electron bombardment using an auxiliary circular tungsten filament and the specimen temperature was monitored with a platinum versus platinum–10% rhodium thermocouple clamped to the graphite post below the specimen. Though the temperature difference between specimen and thermocouple was a function of temperature, heating and cooling curves of the thermo-emf versus time in the vicinity of the specimen melting point (mp) could be used to estimate the uncertainty in the temperature derived from the measured thermocouple-emf. This uncertainty was estimated to be about $\pm 50^\circ\text{C}$ in the vicinity of 660°C (mp for Al) but was larger for higher temperatures. The filament heating current and the heating voltage were supplied from half-wave-rectified power supplies (operating at 60 Hz) and the multiplier pulses were gated so that they were detected only when the heating power was off. The system was normally aligned so that the primary beam impinged in the vicinity of a vertical edge of the specimen though as the specimen size and shape varied it was not readily possible to measure the angle of incidence and the take-off angle. The observed spectra, however, did not vary significantly when specimens of different shape were used with differing positions of the incident beam on the surface except when the scattering angle was small (see below).

III. RESULTS AND DISCUSSION

A. Aluminum

The Al specimen was first heated to about 1100°C at which temperature the surface oxide skin ruptured and dissolved in the liquid Al. The specimen temperature could then be reduced and the specimen maintained in an oxide-free condition essentially indefinitely (as indicated by the presence of the ≈ 10 -eV surface plasmon loss²³), even though the pressure in the vacuum system was $\approx 10^{-6}$ Torr. It is believed that any further oxide formed on the surface went into solution (at a

¹⁸ K. H. Steigerwald, *Optik*, **5**, 469 (1949).

¹⁹ A. E. Ennos, *Brit. J. Appl. Phys.* **4**, 101 (1953); *ibid.* **5**, 27 (1954); H. G. Heide, *Lab. Invest.* **14**, 1134 (1965); **14**, 1140 (1965).

²⁰ J. A. Simpson and L. Marton, *Rev. Sci. Instr.* **32**, 802 (1961); J. A. Simpson, *ibid.* **32**, 1283 (1961).

²¹ E. M. Purcell, *Phys. Rev.* **54**, 818 (1938).

²² M. Hansen, *Constitution of Binary Alloys* (McGraw-Hill Book Co., New York, 1958), 2nd ed.

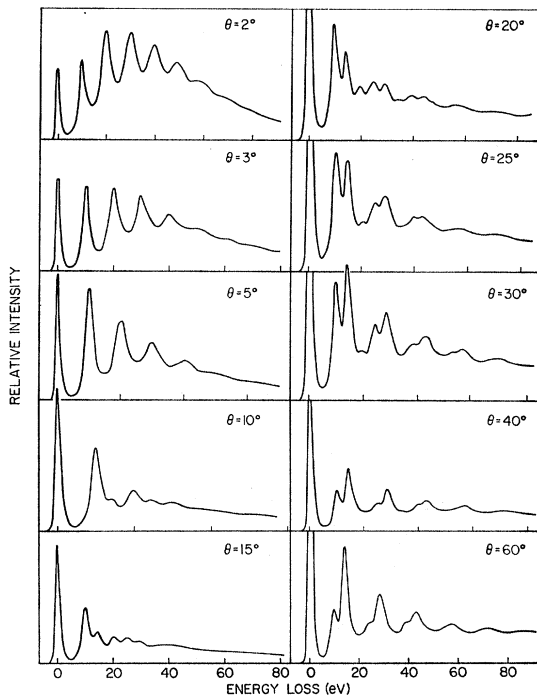


FIG. 3. Characteristic loss spectra of liquid Al for the total scattering angles θ indicated. These spectra have been traced from the original records and no direct comparison can be made between the different intensity scales; note also the different energy loss scales.

very small impurity level). Only after the specimen solidified did the spectra change as oxidation proceeded in the manner reported previously.^{23,24}

A series of characteristic loss spectra for liquid Al are shown in Fig. 3 for various total scattering angles θ . For $\theta = 2^\circ$ the spectrum appears to consist entirely of multiples of a loss of about 10 eV. For larger θ , fewer multiples of the ≈ 10 -eV loss appear and at $\theta = 10^\circ$ a loss at ≈ 15 eV is observed. The latter loss increases in intensity relative to the ≈ 10 -eV loss as θ increases. The spectrum for $\theta = 25^\circ$ is of interest in that the intensities of the ≈ 10 - and ≈ 15 -eV losses are nearly equal while the intensity of the peak at about 20-eV loss, due to electrons which have suffered two ≈ 10 -eV losses, is much less than the intensity of the peak at about 30-eV loss which is due almost entirely to electrons which have suffered two ≈ 15 -eV losses.

Similar intensity variations to those shown in Fig. 3 were observed when the aluminum was allowed to freeze. A small shift in the position of each energy loss was observed at the melting point, as plotted in Fig. 4. When a sufficiently thick layer (~ 1000 Å) of aluminum was evaporated onto the frozen Al, the spectra shown in Fig. 5 were recorded for the scattering angles indi-

²³ C. J. Powell and J. B. Swan, Phys. Rev. **118**, 640 (1960); see also R. L. Hengehold and D. Jones, Bull. Am. Phys. Soc. **10**, 1140 (1965).

²⁴ C. Kunz, Z. Physik **196**, 311 (1966).

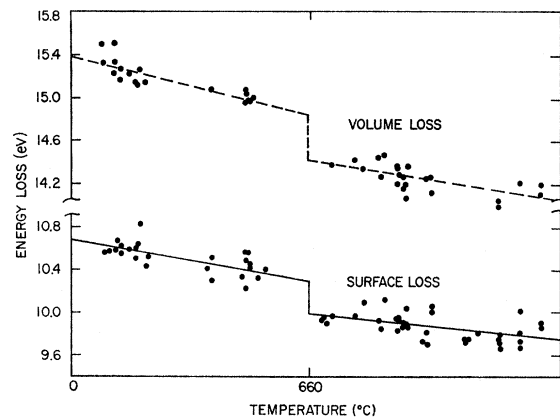


FIG. 4. Measured positions of the volume and surface plasmon losses in solid and liquid Al as a function of indicated emf of the thermocouple on the specimen support. For reasons discussed in Sec. II, only the temperature corresponding to the Al mp (660°C) could be related to the observed thermo-emf. The solid and dashed lines are least-squares straight line fits for the loss values plotted on the thermo-emf scale. The surface and volume losses were measured usually at small- and large-scattering angles, respectively, to maximize the accuracy of location (Fig. 3).

cated. In all such cases, the intensity of the ≈ 15 -eV loss was greater than that of the ≈ 10 -eV loss.

Energy losses at 10.3 and 15.3 eV for evaporated Al specimens have been previously identified^{23,25} as being due to surface plasmon and volume plasmon excitation, respectively. This interpretation is consistent with the analysis of solid Al optical data by Ehrenreich, Philipp, and Segall,²⁶ who find that the only interband transitions with significant oscillator strength occur at transition energies of 1.5 and about 2 eV.

Values of the parameters in Eq. (1) applicable to Al can be derived²⁷ from a least-squares fit to the experimental optical data^{25,28} considering interband transitions in the vicinity of 1.5 and 2 eV and a weak transition near 10 eV. For energies $\hbar\omega$ between 10 and 15 eV, where ω^2 is appreciably greater than g_0^2 , g_f^2 , and ω_j^2 (except for the 10-eV transition), the real part of $\epsilon(\omega)$ is approximately given by the equation

$$\epsilon_1(\omega) \approx 1 - \omega_p^2 (f_0 + \sum_j f_j) / \omega^2.$$

The volume and surface plasmon losses occur at energies $\hbar\omega_v$ and $\hbar\omega_s$ near frequencies for which $\epsilon_1(\omega_v) = 0$ and $\epsilon_1(\omega_s) = -1$, respectively. Thus,

$$\Delta E_v = \hbar\omega_v \approx \hbar\omega_p (f_0 + \sum_j f_j)^{1/2}$$

and

$$\Delta E_s = \hbar\omega_s \approx \hbar\omega_p (f_0 + \sum_j f_j)^{1/2} / \sqrt{2}.$$

Both plasmon losses are proportional to $\hbar\omega_p$ to first order and should show an $N^{1/2}$ variation with temperature [Eq. (2)]. The observed variation of ΔE_v and

²⁵ C. J. Powell and J. B. Swan, Phys. Rev. **115**, 869 (1959).

²⁶ H. Ehrenreich, H. R. Philipp, and B. Segall, Phys. Rev. **132**, 1918 (1963).

²⁷ C. J. Powell (unpublished).

²⁸ M. W. Williams, E. T. Arakawa, and L. C. Emerson, Surface Sci. **6**, 127 (1967).

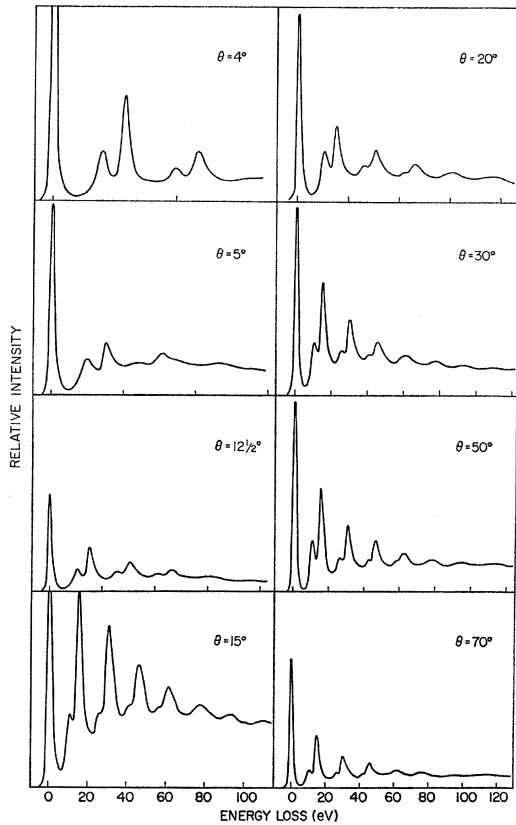


FIG. 5. Characteristic loss spectra recorded when Al was evaporated onto a frozen Al substrate for the scattering angles indicated. Note the different energy-loss scales.

ΔE_s with temperature (Fig. 4) is consistent with the known thermal expansion in the solid²⁹ and liquid¹⁶ phases and with the 6% density change on melting.¹⁶ A similar variation of ΔE_s in solid Al from room temperature to 360°C has been reported previously.³⁰

The change in intensity of the ≈ 10 -eV loss in liquid and frozen Al relative to that of the no-loss peak with scattering angle is in agreement with the variation expected from calculations of the probability for surface plasmon excitation as a function of the scattering geometry.^{6,31} Stern and Ferrell⁶ have shown that the differential probability for the excitation of a surface plasmon at the interface of a medium *A* with $\epsilon_A = 1 - \omega_{pA}^2/\omega^2$ and of medium *B* of dielectric constant ϵ_B can be expressed in the form

$$\frac{dP}{d\Omega} = \frac{e^2}{\pi \hbar v} \frac{2}{(1 + \epsilon_B)} \frac{\theta_E \theta}{(\theta_E^2 + \rho^2)^2} f. \quad (3)$$

In this equation, *v* is the velocity of the primary electron, θ is the scattering angle, and $\theta_E = \Delta E_s/mv^2$. The

²⁹ A. J. C. Wilson, Proc. Phys. Soc. (London) **54**, 487 (1942); F. C. Nix and D. MacNair, Phys. Rev. **60**, 597 (1941).

³⁰ G. Meyer, Z. Physik **143**, 61 (1957); L. B. Leder and L. Marton, Phys. Rev. **112**, 341 (1958).

³¹ A. Otto, Phys. Status Solidi **22**, 401 (1967).

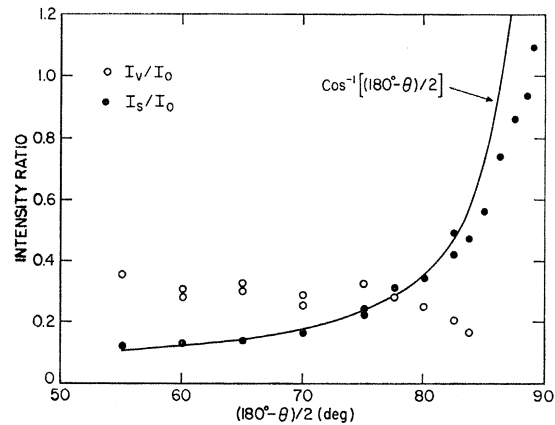


FIG. 6. Plots of the ratio of the surface-plasmon loss peak intensity I_s to the no-loss peak intensity I_0 and of the ratio of the volume-plasmon loss peak intensity I_v to I_0 in liquid Al as a function of $\frac{1}{2}(\pi - \theta)$, where θ is the total electron scattering angle. The solid line is a plot of $\cos^{-1}[\frac{1}{2}(\pi - \theta)]$, normalized to fit I_s/I_0 for the smaller values of $\frac{1}{2}(\pi - \theta)$.

parameter *f* is defined by

$$f^2 = \frac{1 + (\theta_E/\theta)^2}{\cos^2 \alpha} \left(\tan \alpha \cos \chi + \frac{\theta_E}{\theta} \right)^2, \quad (4)$$

where α is the angle of incidence of the electron beam on the surface and χ is the azimuth angle of the scattered beam relative to the plane of incidence. For large α (i.e., small θ), *f* is approximately proportional to $1/\cos \alpha$. The intensity of the surface loss I_s in liquid Al relative to the no-loss peak intensity I_0 is plotted as a function of $\frac{1}{2}(\pi - \theta)$ in Fig. 6 and compared with $\cos^{-1}[\frac{1}{2}(\pi - \theta)]$. The angle of incidence was not defined in the present experiment and the comparison in Fig. 6 is based on the implicit assumption of scattering symmetry (angle of incidence equals angle of "reflection") when $\alpha = \frac{1}{2}(\pi - \theta)$. The similarity between I_s/I_0 and $\cos^{-1}[\frac{1}{2}(\pi - \theta)]$ for $55^\circ < [\frac{1}{2}(\pi - \theta)] < 85^\circ$ is therefore perhaps surprising. For small θ , it is necessary to perform a folding integration of Eq. (3) over the angular variables with limits defined by the scattering geometry³²; changes of about $\pm 10\%$ in I_s/I_0 for small θ were in fact observed for different specimens and different specimen positions.

Otto³¹ has noted that Eq. (4) is invalid in the limit $\alpha \rightarrow 90^\circ$ and has shown that in this limit only surface plasmons are excited. The ratio of the volume loss intensity I_v to I_0 for liquid Al is also shown in Fig. 6 as a function of $\frac{1}{2}(\pi - \theta)$ and it seems that this ratio tends to zero as $\theta \rightarrow 0$. Otto has also given an expression for the excitation probability of the volume plasmon loss as a function of the scattering parameters but it is not possible to compare his result with the observed variation of I_v/I_0 with θ because the electron path distribution in the specimen and its variation with θ are not known.

³² J. Daniels, Z. Physik **203**, 235 (1967).

The variation of I_s/I_0 and of I_v/I_0 with θ is much less marked for the evaporated Al specimens (Fig. 5) than for the liquid and frozen Al. This difference is attributed to the roughness of the evaporated Al surface.³³ It is believed that most of the detected electrons have been transmitted through projections on the surface and that this transmitted fraction is either large for all θ in the present range or does not vary appreciably with θ . By contrast, the liquid and frozen Al surfaces must be relatively smooth. The liquid surface would be expected to be smooth on an atomic scale and since the loss spectra do not change in form on freezing it is inferred that the frozen Al surface must also be smooth on an atomic scale. The extent of the smooth regions and the height of any steps are difficult to estimate though Menzel³⁴ has reported that some near-spherical metal crystals grown by asymmetrical cooling of a liquid drop can be optically smooth over hundreds of microns.

Qualitatively similar variations in the intensities of the surface and volume plasmon losses with scattering angle have been reported by other authors.^{32,35-37} Creuzburg and Raether³⁵ observed different intensities of the surface (I_s) and volume (I_v) losses in diffraction maxima of different orders from a cleaved (111) Si surface, while Lohff³⁶ found different values of I_v and I_s in spectra obtained from rough (mechanically polished) and relatively smooth (electropolished) Al (111) surfaces. These measurements were performed with incident electron energies in the 40- to 50-keV range but Thirlwell³⁷ has observed a variation in I_v and I_s using 200-eV electrons incident on evaporated Al surfaces for scattering angles of 20° and 90°. Daniels³² has recently measured I_s as a function of α ($30^\circ < \alpha < 80^\circ$) for 50-keV electrons transmitted through Ag films and has found a variation similar to that shown in Fig. 6.

The characteristic loss spectra measured in this work reflect all allowed plasmon scattering angles,³⁸ though the shape and the width of the loss peaks should be determined mainly by the more frequent small-angle scattering; that is, there should be no significant broadening of the ≈ 15 -eV Al loss peak measured here on account of the larger breadth found for the larger scattering angles in transmission experiments.³⁹ Von Festenberg,⁴⁰ however, has found larger half-widths at small angles for the ≈ 15 -eV loss peak in Al films with small (≈ 60 -100 Å) crystallite sizes than for large

TABLE I. Measured half-widths (in eV) of the peak of elastically scattered electrons, the surface plasmon peak, and the volume plasmon peak in liquid, frozen, and evaporated Al.

	No-loss peak	Surface-loss peak	Volume-loss peak
Liquid Al	1.4±0.1	2.8±0.2	3.1±0.2
Frozen Al	1.3±0.1	2.6±0.2	2.8±0.2
Evap. Al	1.3±0.1	2.9±0.2	2.5±0.2

crystallite sizes (> 250 Å). This extra damping seems to occur when the plasmon wavelength (a function of scattering angle) is greater than the crystallite size and it has been suggested⁴¹ that the plasmon half-width in liquid Al might be larger than that in the solid Al, on account of the absence of long-range order in the liquid phase. The observed half-widths are shown in Table I and it is seen that though the plasmon half-widths for liquid Al appear to be slightly larger than those for solid Al the differences are comparable to the precision of measurement. The natural width of each plasmon loss peak is estimated to be in the range 1.8-2.3 eV and is appreciably larger than the measured values (0.53-1.05 eV)^{39,40,42} for the small-angle half-width of the ≈ 15 -eV Al loss. From Von Festenberg's work it could be inferred that the crystallite size in the frozen and evaporated Al was ≈ 90 Å but it is not clear whether the half-width of the ≈ 15 -eV loss in liquid Al is related to the lack of long-range order or to possible changes in other parameters on going from the solid to the liquid state (for example, in the dispersion constants which determine the relative number of electrons on the energy-loss scale for various scattering angles).

The close similarity in the loss spectra for liquid and frozen Al suggests that there is no significant change in the spectrum of electronic excitations of Al on melting. This result is in agreement with the prediction of several authors⁴³ that the electronic structure in a condensed phase is determined principally by the short-range order. In the case of Al, there appears to be little change in the coordination number and in the atomic radial distribution function on melting.⁴⁴

Catterall and Trotter⁴⁵ have compared the L_{23} soft x-ray emission spectrum of liquid Al (at about 800-850°C) with that of solid Al and found the spectra for the two phases similar. The structure in the spectrum for liquid Al was less pronounced than that observed in the solid Al spectrum but there was otherwise no significant change in the density of occupied states on melting. Fischer and Baun⁴⁶ observed little change in the K_β emission spectrum of Al as their specimen was melted; at some undetermined temperature above the

³³ J. W. Swaine and R. C. Plumb, *J. Appl. Phys.* **33**, 2378 (1962).

³⁴ E. Menzel, *Rept. Progr. Phys.* **26**, 47 (1963).

³⁵ M. Creuzburg and H. Raether, *Z. Physik* **171**, 436 (1963).

³⁶ J. Lohff, *Z. Physik* **171**, 442 (1963).

³⁷ O. Klemperer and J. Thirlwell, *Solid State Commun.* **4**, 15 (1966); *J. Thirlwell, Proc. Phys. Soc. (London)* **91**, 552 (1967).

³⁸ Based on the cutoff angle for excitation of the ≈ 15 -eV Al volume-plasmon loss by 20-keV electrons [N. Swanson and C. J. Powell, *Phys. Rev.* **145**, 195 (1966)], the corresponding maximum angle for single plasmon scattering with 8-keV electrons would be 1.8°.

³⁹ B. W. Ninham, C. J. Powell, and N. Swanson, *Phys. Rev.* **145**, 209 (1966).

⁴⁰ C. Von Festenberg, *Z. Physik* **207**, 47 (1967).

⁴¹ H. Raether (private communication).

⁴² J. Geiger and K. Wittmaack, *Z. Physik* **195**, 44 (1966).

⁴³ W. D. Knight, A. G. Berger, and V. Heine, *Ann. Phys. (N. Y.)* **8**, 173 (1959); A. F. Ioffe and A. R. Regel, *Progr. Semiconductors* **4**, 237 (1960).

⁴⁴ C. Gamertsfelder, *J. Chem. Phys.* **9**, 450 (1941).

⁴⁵ J. A. Catterall and J. Trotter, *Phil. Mag.* **8**, 897 (1963).

⁴⁶ D. W. Fischer and W. L. Baun, *Phys. Rev.* **138**, A1047 (1965).

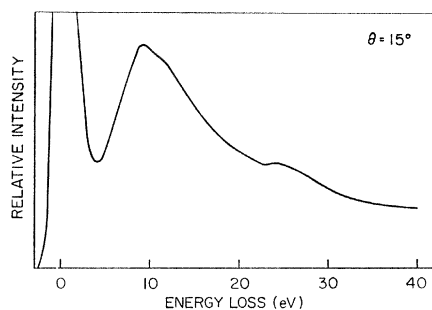


FIG. 7. The characteristic loss spectrum of liquid Bi measured at a scattering angle of 15° .

mp, however, the spectrum changed appreciably and the band width decreased to about half its former value. These latter changes were reversible with temperature.⁴⁷ In the present work, no significant change was found in the form of the liquid Al loss spectra from the mp (660°C) to a specimen temperature estimated from the thermocouple-emf and the onset of appreciable evaporation¹⁷ to be between 1100 and 1200°C .

B. Bi, In, Ga, Hg, and Au

On the basis of the present results for Al, it was considered that satisfactory, oxide-free surfaces of the other liquid elements might be prepared in the same way. That oxide- or contamination-free surfaces had been obtained could be shown for those elements for which a surface plasmon loss was identified (from the angular variation in loss intensity, as in Fig. 6) and observed at a position similar to that found for evaporated specimens which could be shown to be uncontaminated.²³ The spectra for Bi and In could be checked in this way, and the results for the other elements will be separately discussed below. In this phase of the work, loss spectra were usually recorded for three representative scattering angles, low and high values of θ being chosen to enhance the excitation probabilities of the surface and volume plasmon losses (if present), respectively.

1. Bismuth

The characteristic loss spectra of solid and liquid Bi are composed principally of combinations of ≈ 10 - and ≈ 15 -eV losses due to surface plasmon and volume plasmon excitation, respectively.^{12,15} Changes observed in the loss spectra on melting have been described briefly in Sec. IB and elsewhere¹² and have been interpreted in terms of a change in band structure. That a change in band structure in Bi on melting could occur is not surprising since Bi is known to undergo a large change in structure on melting,⁴⁸ compared to other elements. Knight *et al.*⁴⁸ have in fact suggested that the electronic structure of Bi would be significantly different in the solid and liquid states.

⁴⁷ W. L. Baun (private communication).

⁴⁸ H. Hendus, *Z. Naturforsch.* **2a**, 505 (1947).

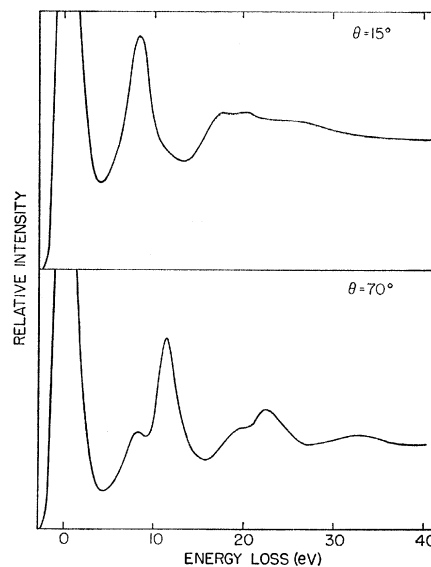


FIG. 8. Characteristic loss spectra of liquid In measured at scattering angles of 15° and 70° .

Further measurements of Bi loss spectra have been performed at a scattering angle of 15° , where the probability of exciting the volume plasmon loss and multiple surface plasmon losses is relatively small. A loss spectrum for liquid Bi is shown in Fig. 7, where a broad peak centered at about 26.6 -eV energy loss is found in addition to the surface plasmon loss peak and an interband transition¹² at 11.5 eV. A peak of the same shape and relative magnitude is also observed at 26.6 eV when the bismuth was solidified. Minima in the transmittance of Bi films have been reported⁴⁹ at photon energies of 24.6 and 27.6 eV and these and the 26.6 -eV loss peak found here are considered to be due to excitation of electrons from the O_4 and O_5 subshells (with binding energies relative to the Fermi level of 26.5 and 24.4 eV, respectively).⁵⁰

Loss spectra were also measured for Bi evaporated onto frozen Bi for scattering angles $\theta = 6^\circ$, 40° , and 70° . No significant change in the spectra with θ was observed, as with Al (Fig. 5), and the spectra were similar to those found for frozen Bi at $\theta = 70^\circ$.¹²

2. Indium

As with Bi,¹² the indium specimen was initially heated about 200°C above the melting point (156°C) to eliminate the surface oxide; strong surface plasmon loss peaks could then be observed. Measurements of the loss spectra were made for $\theta = 15^\circ$, 40° , and 70° and typical spectra are shown in Fig. 8. The surface and volume plasmon loss peaks were observed to vary in intensity with scattering angle and to occur at 8.2 ± 0.2 and 11.5 ± 0.2 eV, respectively. Robins⁵¹ has reported

⁴⁹ W. R. Hunter, D. W. Angel, and R. Tousey, *Appl. Opt.* **4**, 891 (1965).

⁵⁰ J. A. Bearden and A. F. Burr, *Rev. Mod. Phys.* **39**, 125 (1967).

⁵¹ J. L. Robins, *Proc. Phys. Soc. (London)* **79**, 119 (1962).

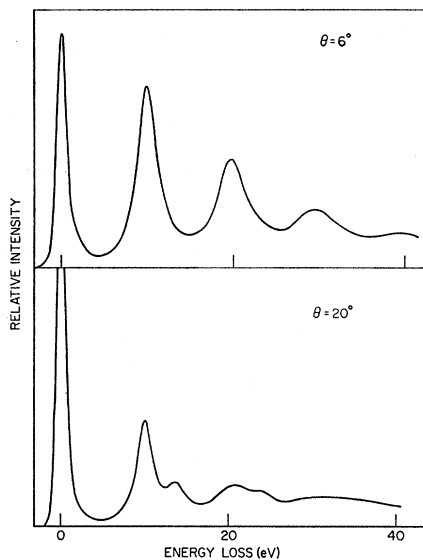


FIG. 9. Characteristic loss spectra of liquid Ga measured for scattering angles of 6° and 20° .

surface and volume plasmon energy losses in evaporated In specimens of 8.7 ± 0.1 and 11.3 ± 0.1 eV. In addition, the spectrum for $\theta = 15^\circ$ showed a broad energy loss peak in the vicinity of 20 eV. Wilson and Rice¹⁴ have reported structure in the reflectivity of liquid In in the same photon energy region and it appears that this structure may be associated with the excitation of electrons from the $N_{4,5}$ levels, the binding energy being 16.2 eV.⁵⁰ Increased optical absorption beginning at about 16.5 eV in solid In has been reported by several authors.⁵²

The In loss spectra changed before solidification, presumably due to surface contamination or to precipitation of the oxide in solution. The surface plasmon loss shifted (continuously) to 7.5 ± 0.2 eV,⁵³ the volume plasmon loss position remained unchanged, and a very broad loss appeared at about 22 eV; no further change occurred on solidification. Any change in plasmon loss position due to the 2.5% density change on melting,¹⁶ however, would not be greater than the precision of measurement.

3. Gallium

The gallium specimen was first heated to about 400°C and loss spectra were recorded for $\theta = 6^\circ$ and $\theta = 20^\circ$ (Fig. 9). The spectra consisted entirely of multiples of losses of 9.9 ± 0.2 and 14.2 ± 0.3 eV, identified as surface and volume plasmon losses, respectively, on the basis of variation of loss intensity with θ . Robins⁵¹ observed losses of 10.2 ± 0.1 and 13.9 ± 0.1 eV in evaporated Ga and made a similar identification. Gallium is also known

⁵² W. C. Walker, O. P. Rustgi, and G. L. Weissler, *J. Opt. Soc. Am.* **49**, 1471 (1959); W. R. Hunter, *J. Phys. (Paris)* **25**, 154 (1964).

⁵³ The 7.5-eV loss is an indium surface plasmon loss that occurs instead of the 8.2-eV loss when oxide or contamination is present (cf. Refs. 6, 23, and 24).

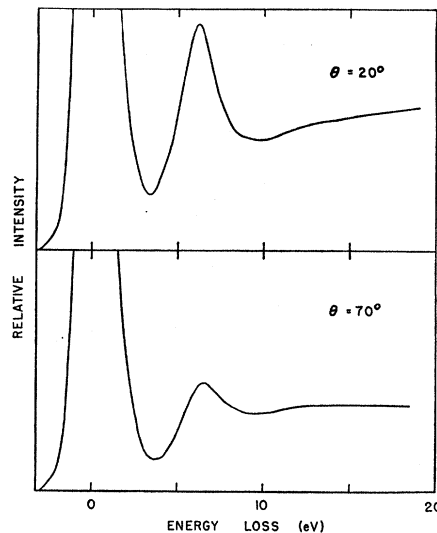


FIG. 10. Characteristic loss spectra of liquid Hg measured at scattering angles of 20° and 70° .

to undergo a relatively large change in structure on melting⁴⁸ and an increase in density,¹⁶ like Bi, but the present results for liquid Ga and Robins's results for solid Ga are not significantly different. If, however, there was a difference in the solid and liquid spectra comparable to that found for Bi, it would be desirable to compare spectra obtained under the same scattering conditions. Unfortunately, it was not possible to study solid Ga in the present experiment because the liquid surface was apparently contaminated before solidification, the surface loss decreasing continuously to about 8.8 eV.

4. Mercury

It was not possible to heat the mercury specimen above room temperature without significant evaporation and since no other method for generating a clean surface was readily available the observed spectra (Fig. 10) do not necessarily represent an uncontaminated Hg surface. Nevertheless, the spectra recorded for $\theta = 70^\circ$ show a loss at 6.5 ± 0.1 eV, which is close to the position expected for the volume plasmon loss from the optical data of Wilson and Rice¹⁴ and the spectra for $\theta = 20^\circ$ show a loss at 6.2 ± 0.1 eV. This apparent shift could be due to an unresolved intensity contribution from the surface plasmon loss which would be

TABLE II. Positions (in eV) of the energy loss peaks in liquid, frozen, and evaporated Au for scattering angles θ of 5° and 40° . The errors shown are mainly estimates of the uncertainties in peak locations due to peak overlap.

Form	θ	Energy-loss values (eV)			
Liquid	5°	5.4 ± 0.4		17.1 ± 0.7	22.8 ± 1
Liquid	40°	6.6 ± 0.4	9.2 ± 1	17.1 ± 1	25.5 ± 1
Frozen	5°	5.6 ± 0.4		17.5 ± 0.7	23.6 ± 1
Frozen	40°	6.3 ± 0.3	9.8 ± 0.5	17.1 ± 0.5	25.0 ± 1
Evap.	40°	6.2 ± 0.5	10.8 ± 0.5	16.3 ± 0.5	24.8 ± 1
					33.2 ± 2

expected¹⁴ to occur at about 6 eV. The observed loss of 6.5 eV for $\theta=70^\circ$ agrees well with the value of 6.4 ± 0.1 eV reported by Boersch *et al.*¹⁰ from transmission measurements with liquid Hg though the loss of 10.8 eV found by these authors is not observed in the present experiment.

5. Gold

Many measurements have been made of electron energy loss spectra⁵⁴⁻⁵⁸ and of optical constants⁵⁹⁻⁶⁶ with gold specimens though in many cases there have been large disagreements between the results of different authors. For example, Beaglehole⁶¹ has checked the data of Canfield *et al.*⁶⁰ for internal consistency and has claimed that the structure reported by these authors in the 16- to 24-eV region is spurious. Creuzburg,⁵⁷ however, has derived $-\text{Im}(1/\epsilon)$ from an electron energy loss spectrum and found close agreement with the shape of the $-\text{Im}(1/\epsilon)$ curve determined by Canfield *et al.*, particularly in the disputed 16- to 24-eV range, though Creuzburg's values of $-\text{Im}(1/\epsilon)$ are almost double those of Canfield *et al.* There are considerable variations in the positions of the electron loss peaks for Au and in the relative intensities of the several peaks when measured under apparently similar conditions.⁵⁴⁻⁵⁸ Most of these experiments were performed with evaporated specimens, as were many of the optical measurements. It has recently become clear that the optical properties of evaporated gold films in the visible and near-ultraviolet spectral regions depend on the deposition parameters, such as speed of evaporation, substrate temperature, and film thickness.⁶³⁻⁶⁶ These variations in the optical constants have been correlated with structure changes in the specimens.⁶⁵ Such factors may account for differences in optical constants mea-

sured with evaporated films compared to those for bulk specimens and for variations in the results of different authors using evaporated films in either optical or electron energy loss experiments. In addition, Carillon and Gauthé⁵⁸ have observed different energy loss spectra for evaporated Au films measured before and after heat treatment in air and which have been interpreted by them in terms of carbonaceous contamination introduced in the specimen at the time of preparation.

Because of the relative complexity of the gold loss spectra (e.g., compared to Al) and the apparent discrepancies in published loss spectra and optical constants which may be at least partly due to structure variations or specimen impurities, it is not possible to make a satisfactory identification of the observed energy loss structure. Nevertheless, there appear to be at least several interband transitions between 2 and 40 eV.⁶⁰⁻⁶² The admixture of the contribution of these transitions with the free-electron contribution to $\epsilon(\omega)$ is such that between approximately 6 and at least 27 eV, ϵ_1 is approximately 0.5. Even though ϵ_2 is between 1 and 3 in this photon energy range, relatively broad structure in $-\text{Im}(1/\epsilon)$ may occur at more than one energy which has the character of a volume plasmon loss.⁹ In such cases, one cannot separately identify structure in energy loss spectra as being solely due to interband transitions or to plasmon excitation.

In this work, electron energy loss spectra were recorded with liquid Au at a temperature estimated to be within 100°C of the mp (1063°C) and with frozen Au at a temperature usually between 250 and 500°C. Measurements were made for scattering angles of 5° and 40° and typical spectra are shown in Fig. 11. In addition, gold was evaporated onto the frozen Au and a typical spectrum for $\theta=40^\circ$ is shown in Fig. 12; similar spectra were recorded for $\theta=5^\circ$ though the inelastic signal was smaller. The average loss values are given in Table II.

The loss spectra for liquid and frozen Au are generally similar, at each scattering angle, though there are some significant differences. The 34.2-eV energy loss peak in the spectrum of frozen Au for $\theta=40^\circ$ is not distinguishable in the liquid Au spectrum for $\theta=40^\circ$, and the structure at 9.8 and at 17.7 eV in the frozen Au spectrum is much less pronounced in the liquid spectrum. The shape of the liquid Au spectrum for $\theta=40^\circ$, however, is very similar to that of the frozen Au spectra, and it appears that the same inelastic processes occur in the liquid as in the solid. The change in the loss spectrum on melting can be interpreted in terms of a broadening of the loss peaks, though as the spectra for both liquid and frozen Au consist of relatively broad overlapping peaks, it is not readily possible to estimate half-widths or changes in half-widths of the components. Such broadening of the loss peaks on melting corresponds to hypothesis (d) described in Sec. I B.

⁵⁴ J. L. Robins, Proc. Phys. Soc. (London) **78**, 1177 (1961). This paper contains a summary of earlier measurements of gold energy-loss spectra.

⁵⁵ C. Gout, F. Pradal, and R. Simon, Compt. Rend. **254**, 1233 (1962).

⁵⁶ O. Sueoka and F. Fujimoto, J. Phys. Soc. Japan **20**, 569 (1965); H. Fukutani and O. Sueoka, *ibid.* **20**, 620 (1965).

⁵⁷ M. Creuzburg, Z. Physik **196**, 433 (1966).

⁵⁸ A. Carillon and B. Gauthé, Compt. Rend. **263**, 1242 (1966).

⁵⁹ M. Otter, Z. Physik **161**, 539 (1961).

⁶⁰ L. R. Canfield, G. Hass, and W. R. Hunter, J. Phys. **25**, 124 (1964).

⁶¹ D. Beaglehole, Proc. Phys. Soc. (London) **85**, 1007 (1965). I am indebted to Dr. Beaglehole for a table of his values of ϵ_1 and ϵ_2 .

⁶² B. R. Cooper, H. Ehrenreich, and H. R. Philipp, Phys. Rev. **138**, A494 (1965). Note that the Au optical constants and $-\text{Im}(1/\epsilon)$ determined from a Kramers-Kronig analysis of the normal incidence reflectivity data of Canfield *et al.* (Ref. 60) by these authors differs by $\sim 10\%$ from the corresponding values derived by Canfield *et al.* from reflectivity data at several angles of incidence.

⁶³ N. Emeric and A. Emeric, Compt. Rend. **260**, 845 (1965); N. Emeric, A. Emeric, and R. Philip, J. Phys. **26**, 769 (1965).

⁶⁴ P. Rouard, Appl. Opt. **4**, 947 (1965).

⁶⁵ J. E. Davey and T. Pankey, J. Appl. Phys. **36**, 2571 (1965).

⁶⁶ R. Philip, J. Phys. Radium **20**, 535 (1959); W. Flechsig, Z. Physik **162**, 570 (1961); H. Mayer and H. Bohme, J. Phys. (Paris) **25**, 81 (1964); R. Payan and G. Rassigni, *ibid.* **25**, 92 (1964).

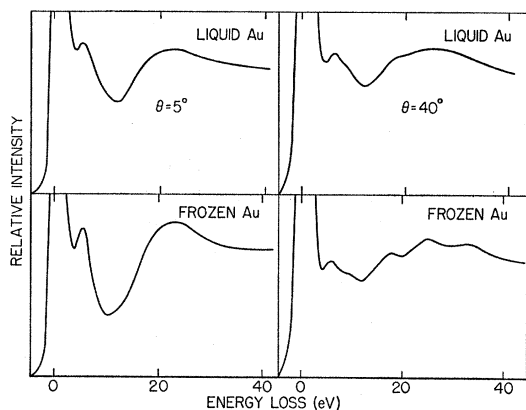


FIG. 11. Characteristic loss spectra for liquid Au (top) and frozen Au (bottom) for scattering angles of 5° (left) and 40° (right). The asymmetry in the no-loss peak is due to unresolved small-energy-loss scattering.

The Au spectra for $\theta = 5^\circ$ in Fig. 11 differ from those for $\theta = 40^\circ$ in three ways. Firstly, the peak at 34.2-eV loss in the frozen Au spectrum at $\theta = 40^\circ$ is not visible in the spectrum for $\theta = 5^\circ$ though there may be a "shoulder" or asymmetry on the high-energy loss side of the ≈ 25 -eV peak. Because of the reduced intensity of the 34.2-eV loss, the maximum of the ≈ 25 -eV loss observed at $\theta = 40^\circ$ is shifted to ≈ 23 eV; this apparent shift is related only to a change in the "background" due to neighboring peaks. Secondly, the intensity of the structure located at ≈ 5.5 eV in both frozen and liquid Au for $\theta = 5^\circ$ is much greater than the intensity of the structure at ≈ 6.4 eV observed in both phases for $\theta = 40^\circ$. These changes in relative intensity of the structure in the ≈ 6 - and ≈ 34 -eV regions with scattering angle are not as marked as the intensity changes of the ≈ 10 - and ≈ 15 -eV losses in Al (Figs. 3 and 6) but they and the limited optical data suggest that the structure at ≈ 34 -eV loss in frozen Au for $\theta = 40^\circ$ is associated with volume plasmon excitation and that there is a surface plasmon excitation occurring at an energy loss less than 6 eV. Creuzburg⁵⁷ has reported evidence for a surface plasmon loss at about 2.5 eV though it is not possible, for reasons discussed above, to ascribe exclusively any loss in a spectrum with as much structure as that of Au to plasmon excitation [as may be done in solids for which the last term in Eq. (1) is negligible in the frequency range of interest].⁹ Finally, the structure at 9.8-eV loss in the frozen Au spectrum for $\theta = 40^\circ$ is not visible at $\theta = 5^\circ$ and the prominent structure at 17.1 eV in the $\theta = 40^\circ$ spectrum is barely detectable in the $\theta = 5^\circ$ spectrum for frozen Au. These loss peaks may also be associated with volume plasmon excitation in the limited sense just mentioned.

Some variability was observed in the "contrast" of the loss peaks for frozen Au on different runs, the ratio of intensity at a peak maximum to that of a neighboring minimum varied up to about 10%. It appeared that the half-widths of the peaks changed, presumably as a

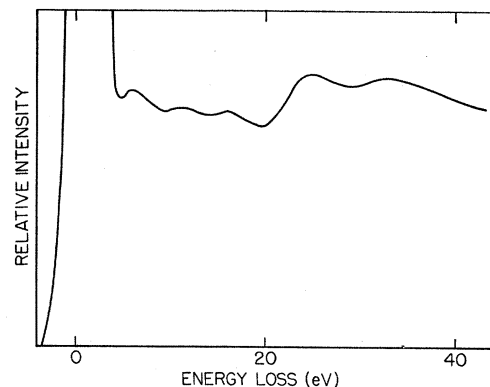


FIG. 12. Characteristic loss spectrum for Au evaporated onto a frozen Au substrate at a scattering angle of 40° .

result of structure changes or variations after freezing. The rate of temperature change during freezing and the time at which the specimen was at a sufficiently high temperature for annealing were not controlled.

The spectrum of gold evaporated onto frozen gold, shown in Fig. 12, is quite different from that of frozen Au for $\theta = 40^\circ$. Peaks are observed at essentially the same positions (considering possible shifts in apparent peak positions due to change in the background from tails of nearby peaks) though the peak intensity ratios differ considerably. In particular, the peaks located at about 10.8- and 16.3-eV energy loss appear much more intense than corresponding peaks in the frozen Au spectrum for $\theta = 40^\circ$. The increased intensity for these two losses may be additional evidence that they are associated with volume plasmon excitation (cf. Figs. 3 and 5), with intensity dependent on the surface topography. Alternatively, the differences in the spectrum for evaporated and frozen Au at $\theta = 40^\circ$ together with the variations in relative intensities observed in the frozen Au spectra may be due to structure differences of the type that have been correlated with variations in the optical constants.⁶⁵

It might be expected that variations in peak widths in the frozen Au spectra and the apparent increases in peak widths on melting could be interpreted in terms of variations and increases in disorder, respectively. Heating the evaporated Au to an annealing temperature led to the appearance of a minimum in the vicinity of 12-eV loss like that observed for frozen and liquid Au at $\theta = 40^\circ$.

The variations in relative peak intensities in the Au spectra recorded under different conditions are typical of the variations in published gold spectra.⁵⁴⁻⁵⁸ The spectra shown here, however, are similar in general to these found in most previous measurements. Since gold is relatively inert chemically, it seems that the observed variations can only be interpreted by variations in specimen topography and local scattering geometry or by defects in the bulk introduced at the time of preparation. In the future, it would be desirable

to prepare specimens for energy loss or for far-uv optical experiments in the same way as in studies⁶⁷ of nucleation, growth and disorder characteristics of evaporated Au films so that the variable structure for excitations greater than 6 eV can be more fully investigated. In addition, it would be interesting to measure the peak widths in evaporated Au films with varying crystallite sizes as a function of scattering angle, as Von Festenberg has done for Al.⁴⁰

Otter⁶⁷ has measured the optical constants of solid Au at various temperatures between 10°C and the mp and of liquid Au at the mp for photon energies between about 2 and 3 eV. He used the Menzel³⁴ technique for generating smooth, clean surfaces, similar to that used here. Otter's results show that the rise in ϵ_2 with increasing photon energy at about 2.5 eV became less pronounced as the temperature was raised; for liquid Au, the maximum in ϵ_2 is small and ϵ_2 is large over the measured energy range. The energy resolution in the present work was not sufficient to see if related changes occurred in the electron loss spectra.

IV. SUMMARY

In this work, characteristic electron energy loss spectra for liquid Al, Bi, In, Ga, Hg, and Au have been described. Where possible (Al, Bi, and Au), the loss spectra for the frozen solid have been obtained under otherwise similar scattering conditions and compared with those for the liquid state; in all three cases, the loss spectra changed reversibly as the specimen was interchanged between the solid and liquid phases. In addition, loss spectra for Al, Bi, and Au evaporated onto frozen Al, Bi, and Au, respectively, have been described.

Several hypotheses have been discussed in the Introduction as to how the loss spectrum of a solid might be expected to change when the sample was liquefied. The energy losses in Al varied with temperature and changed at the mp in a manner that could be interpreted entirely in terms of known density variations. Changes occurred in the Bi loss spectra on melting which were indicative of a change in interband transition energies and hence in band structure.¹² That such a band structure change might occur is not unexpected because the short-range order in Bi changes significantly on melting.⁴³ Peaks in

the loss spectra for Au appeared to become broader and less distinct on melting; such changes were interpreted in terms of decreased lifetimes of the excited states with increased disorder. The loss spectra for the three liquid elements, however, were generally similar to those for the corresponding solids and the main conclusion of this work is that there does not appear to be a drastic change in the electronic structure of these elements on melting. That is, the electronic structure appears to be determined principally by the short-range order.⁴³

The spectra for liquid In and Ga were similar to those obtained using evaporated specimens. Since Ga is also known to undergo a significant structure change on melting, it would be desirable to measure the spectra for liquid and solid Ga in the same apparatus so that any difference could be more clearly observed. The liquid Hg spectrum was found to be consistent with recent optical data.¹⁴

The spectra for the liquid and frozen samples in this work varied with scattering angle, because of the varying probabilities for surface- and volume-plasmon excitation with geometry and electron penetration. As noted also by Thirlwell and Klemperer,³⁷ this variation can be used as a means to identify the loss mechanism, in addition to those used previously.^{2,15}

In this work, a technique very similar to that developed by Menzel³⁴ has been used to generate the experimental surfaces. Compared to other means of generating clean surfaces, this technique is relatively simple and convenient; in addition, the surfaces are atomically smooth over distances estimated to be at least several hundred angstroms. By contrast, the spectra for evaporated specimens show that the surfaces are rougher than the frozen surfaces, as might be expected. The general agreement between the spectra shown here and these measured for evaporated specimens, particularly in the position of the surface plasmon loss which is sensitive to surface contamination,^{23,24} indicates that there was no significant specimen contamination from either the residual atmosphere or the specimen support.

ACKNOWLEDGMENTS

The author wishes to thank Dr. J. A. Simpson, Dr. R. D. Young, and his other colleagues for suggestions and discussions during the course of this work. He is also indebted to A. B. Dausies and L. E. Mann for their excellent work in the construction of the apparatus.

⁶⁷ C. A. Neugebauer, in *Physics of Thin Films*, edited by G. Hass and R. E. Thun (Academic Press Inc., New York, 1964), Vol. 2, p. 1; D. W. Pashley, *Advan. Phys.* 14, 327 (1965); H. Viethaus, *Z. Naturforsch.* 22a, 2123 (1967).